Proc. Natl. Acad. Sci. USA
Vol. 79, pp. 5718–5722, September 1982
Neurobiology

Perforated postsynaptic densities: Probable intermediates in synapse turnover

(subsynaptic plate perforations/postsynaptic perforations/synapse replacement/hippocampal formation)

M. NIETO-SAMPEDRO, STEVEN F. HOFF, AND CARL W. COTMAN

Department of Psychobiology, University of California, Irvine, California 92717

Communicated by Richard F. Thompson, May 27, 1982

ABSTRACT **The molecular layer of the dentate gyrus of normal rats shows a large incidence of perforated postsynaptic densities (PSDs). The perforations or discontinuities occur almost exclusively in PSDs located in spines showing a U- or W-shaped junctional profile (complex PSDs). Perforated PSDs account for 16–25% of the total complex PSD profiles in young adult rats and 12–29% of those in aged animals. The frequency of perforations in the inner molecular layer of the dentate gyrus undergoes significant changes during a cycle of nondegenerative synapse turnover induced by ipsilateral ablation of the entorhinal cortex. During the first 2 days postlesion nonperforated PSDs (simple PSDs) decrease sharply, whereas perforated PSDs change little. However, at later times (4–10 days) there is a significant increase in the number of perforated PSDs that balances the number of simple PSDs lost. Beyond 10 days postlesion the proportion of both types of PSD is restored slowly to normal—i.e., nonperforated PSDs increase in number and perforated PSDs decrease, returning to the values in unoperated animals by 120 days postlesion. This inverse relationship between small nonperforated PSDs and large perforated PSDs suggests a precursor–product relationship between them. We propose that perforated PSDs are intermediates in an ongoing cycle of synapse turnover that is a part of the normal maintenance and adaptation of the nervous system.**

Synapse replacement (synapse turnover) appears to be part of the normal program both for the maintenance of the peripheral and central nervous systems of adult vertebrates and for their adaptation to changing situations. Experimental evidence for the existence of this process is widespread (reviewed in refs. 1 and 2) but indirect, depending on inferences derived from the observation of characteristic degenerating and regenerating synaptic profiles. In normal animals the proportion of these profiles is generally small and furthermore, synapse turnover may occur without display of such structures. Perhaps the greatest difficulty in studying synapse turnover in the adult is to devise a method to trigger it reliably in a statistically meaningful neuronal population. We have found that unilateral lesions of the entorhinal cortex initiate a cycle of synapse turnover in areas of the hippocampal formation that do not receive afferent input from the injured cortex (3, 4). The replacement of synapses thus induced is similar to the natural turnover process in unoperated animals in that degenerating profiles are never observed and synapse disconnection does not require the loss of either axonal or dendritic counterparts. However, an advantage with respect to the natural process is that synapse turnover can be elicited at will in a large synapse population and studies on the intermediate stages are possible. Here, we report the use of this method to study the structural changes that occur in the postsynaptic densities (PSDs) of asymmetric synapses in the hippocampal dentate gyrus during one cycle of synapse turnover.

PSDs are submembrane structures present in all synaptic junctions and particularly prominent in so-called Gray's type I (5), or asymmetric (6), synapses. The overall shape of PSDs is that of disks with maximum diameter ranging from about 100 to 900 nm (7). In transmission electron microscopy of tissue sections, PSD disks appear either as straight bars of electron dense material (simple synapses; ref. 8) or as U-shaped or W-shaped profiles (complex synapses; ref. 8). In addition, Peters and Kaisermann-Abramof (7) observed that the larger PSDs frequently have one or more perforations. The presence of perforations was confirmed by Cohen and Siekevitz (9) and could also be observed in PSDs purified by subcellular fractionation (10) in all vertebrate species examined from gelatinous fish to mammals (11). It has been proposed that perforations act as a device to increase the transmitting surface of a junction by increasing the surface of PSD edges (7). Others postulate that PSDs are involved in controlling the signal generated by neurotransmitter reception (12). In this case, perforations have been visualized as the static representation of holes that *in vivo* are continuously opening and closing (10). The evidence presented in this paper suggests an alternative view—namely, that perforations probably represent intermediate stages in the turnover of synapses and their PSDs.

MATERIALS AND METHODS

Sprague–Dawley male albino rats were used and, unless indicated otherwise, were 90 days old at the initiation of the experiment. The methods used for ablation of the entorhinal cortex, perfusion, preparation of the hippocampal dentate gyrus for quantitative electron microscopy, and measurement of synapse number have all been reported (3, 4). Average dimensions of PSDs were measured by using a Zeiss MOP-3 digital image analyzer.

RESULTS

Organization of the Dentate Gyrus Molecular Layer. The molecular layer of the dentate gyrus (DML) in the hippocampal formation of the rat was chosen for this study because previous work from our and other laboratories has characterized in detail the synaptology and reactive synapse turnover in this brain region (2–4, 13–15). For the purposes of the present report, the DML will be considered as divided into three equally wide layers: the closest to the granule cell layer is called inner molecular layer (IML); moving towards the hippocampal fissure is the second one-third, or middle molecular layer (MML); next to the fissure is the outer molecular layer (OML). The IML is inner-

The publication costs of this article were defrayed in part by page charge payment. This article must therefore be hereby marked "*advertisement*" in accordance with 18 U. S. C. §1734 solely to indicate this fact.

Abbreviations: PSD, postsynaptic density; DML, molecular layer of dentate gyrus; IML, MML, and OML, inner, middle, and outer layers of dentate gyrus, respectively.

vated primarily by commissural/associational axons from hippocampal area CA4, whereas most of the input to the MML and OML originates in the ipsilateral entorhinal cortex. Sometimes MML and OML are described as a unit, referred to as the outer two-thirds of the molecular layer.

Classification of Synapses. The large majority of the synapses in the DML are located on dendritic spines and according to their overall shape they have been classified into simple (previously called "non-complex") and complex (3, 8, 15). Simple synapses were generally asymmetric (≈90%), and in ultrathin sections their PSDs appeared as rather short straight bars (Fig. 1*A*; average length = 201 nm; SD = 68 nm; n = 828). Longer PSDs were occasionally seen in simple synapses (Fig. 1*B*), and their frequency increased in the IML after ipsilateral entorhinal ablation (see below). The PSDs of complex synapses were longer (average length = 370 nm; SD = 86 nm; n = 232) and their sections were U-shaped or W-shaped (Fig. 1 *C–F*). In the DML of normal rats, complex synapses accounted for about 16% of the total synapse population (14.5% U-shaped; 1.4% W-shaped). Complex synapses always display a negative curvature using the terminology of Dyson and Jones (16)—that is, PSDs are concave when observed from the presynaptic terminal. Synapses with a positive curvature were exceedingly rare in the DML of adult animals but occasionally were seen near the hippocampal fissure. The PSDs of 71–85% of the complex synapses observed in thin tissue sections were continuous curved bars, as in Fig. 1*C*, but 15–29% of the PSDs exhibited discontinuities of various sizes (Fig. 1*D* and *E*). These discontinuities are denominated perforations (7) but at least some of them could equally well correspond to furrows or indentations in the PSD structure. The perforations were sometimes so large that the cytoplasm protruded through them, conferring on the synapse a W-like shape (Fig. 1*F*). Coated vesicles were frequently seen associated with W-type PSDs. Three-dimensional reconstructions from serial sections of synapses appearing to have two or more PSDs have been shown to consist of a single PSD with one or more perforations (7). In this study only those PSDs showing a clear discontinuity, as shown in Fig. 1, are considered perforated. Perforations are observed only in asymmetric synapses.

Perforations in PSDs in the Dentate Gyrus of Unoperated Animals. The proportion of perforated PSDs in the DML of normal animals is shown in Table 1. PSDs in simple synapses rarely were perforated (<1%), but the fraction of perforated PSDs in complex synapses was very high (15–29%). Taking into account that the probability of sectioning a PSD across one perforation cannot be higher than about 21% (50- to 70-nm section thickness/370-nm average diameter of complex PSD), it seems very likely that most complex PSDs carry one or more perforations or similar discontinuities. The average diameter of simple PSDs was 201 nm (SD = 68 nm; n = 828), compared to 321 nm (SD = 80 nm; n = 151) for nonperforated complex PSDs and 460 nm (SD = 96 nm; n = 81) for perforated complex PSDs. The appearance of perforations correlated significantly (two-tailed Student's t test) with both the maximum diameter of the PSD and with the shape of the PSD (shape: complex vs. simple, $P < 0.001$, $t = 7.3717$, df = 6; diameter: Wilcoxon test for large samples, simple vs. complex, $z = 15.06$, $P < 0.0000001$). This correlation, as well as the ratio of complex to total synapses, was maintained throughout the life span of adult animals (Table 1). The distribution of complex PSDs throughout the molecular layer was not homogeneous—i.e., complex PSDs frequently occurred in clusters interspersed in areas free of them.

PSD Perforations After Unilateral Entorhinal Lesion: Ipsilateral IML. Unilateral ablation of the entorhinal cortex does not denervate the IML of the ipsilateral dentate gyrus (13). However, the synapses in this zone undergo a transient nondegenerative disconnection and subsequent reassembly (one cycle of synapse turnover; refs. 2 and 3). Closer examination of the time course of synapse loss and of the type of synapses lost (Fig. 2) showed that only simple synapses were missing,

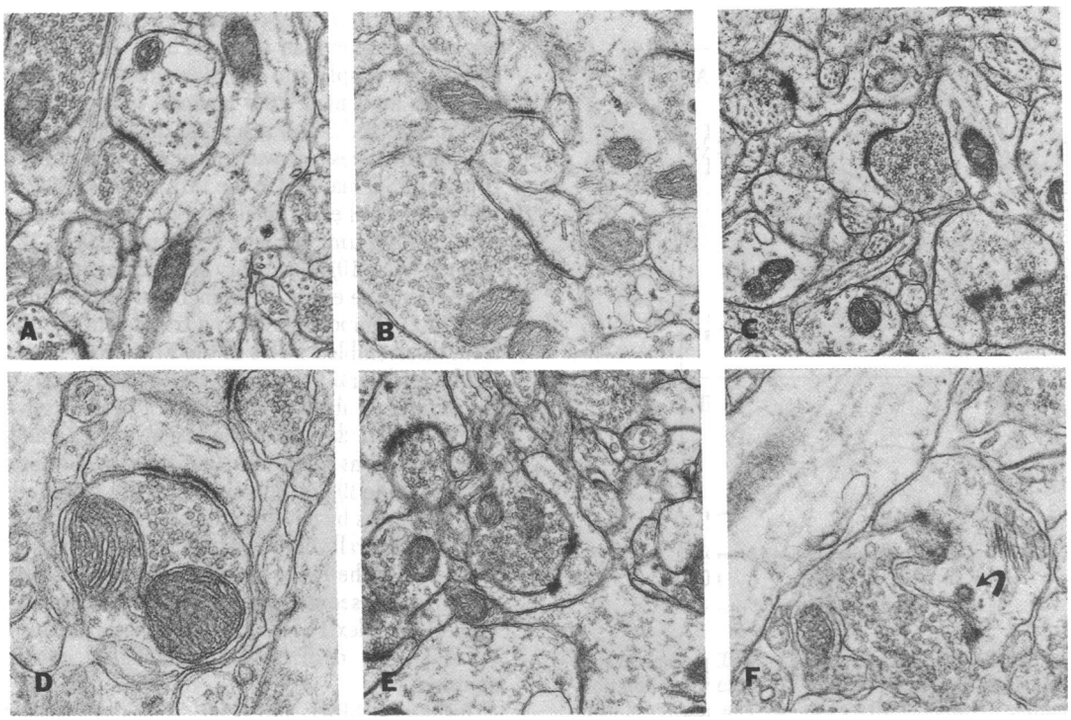

FIG. 1. Different types of asymmetric synapses in the rat DML. (*A*) A typical simple PSD disk with a short diameter. (×20,600.) (*B*) Large simple PSDs were quite infrequent in nonoperated animals and became more abundant 2–4 days postlesion. (×20,600.) (*C*) The majority of complex PSDs were U-shaped and showed no perforations. (×18,300.) However, a significant proportion of them showed one or more perforations of various sizes (*D*, ×24,900; *E*, ×18,200). The discontinuities in some PSDs were very large and the cytoplasm protruded through them (*F*, ×25,600). Large perforations or discontinuities were found in W-shaped spines, and coated vesicles (arrow) were frequently associated to them.

Table 1. Perforations in the PSDs of the molecular layer of the rat dentate gyrus

	IML	MML	OML
	3 month old (4 rats)		
Simple synapses, no./100 μm^2	26.3 ± 1.6	29.8 ± 2.2	31.1 ± 2.5
PSD diameter, nm	197 ± 57	204 ± 93	202 ± 57
	(260)	(263)	(305)
Fraction perforated	0.004 ± 0.002	0.002 ± 0.002	0.005 ± 0.004
Complex synapses, no./100 μm^2	4.8 ± 0.7	5.2 ± 1.1	6.4 ± 1.5
PSD diameter, nm	386 ± 100	352 ± 77	375 ± 84
	(58)	(80)	(94)
Fraction perforated	0.25 ± 0.04	0.21 ± 0.02	0.16 ± 0.07
Complex synapses, % of total	16	15	17
	24 month old (4 rats)		
Simple synapses, no./100 μm^2	24.6 ± 1.3	26.0 ± 1.3	23.6 ± 1.7
Fraction perforated	0	0.0007 ± 0.0007	0.037 ± 0.019
Complex synapses, no./100 μm^2	6.5 ± 1.0	8.3 ± 0.6	6.5 ± 0.7
Fraction perforated	0.29 ± 0.07	0.21 ± 0.01	0.23 ± 0.03
Complex synapses, % of total	21	24	22
	30 month old (5 rats)		
Simple synapses, no./100 μm^2	21.4 ± 2.4	24.6 ± 1.9	22.8 ± 2.0
Fraction perforated	0.0033 ± 0.002	0.0052 ± 0.0052	0.023 ± 0.011
Complex synapses, no./100 μm^2	3.7 ± 0.9	6.7 ± 1.8	6.2 ± 1.6
Fraction perforated	0.25 ± 0.10	0.12 ± 0.05	0.13 ± 0.04
Complex synapses, % of total	15	21	21

For analysis, the dentate gyrus molecular layer was divided into thirds: IML, MML, and OML (see text). Values are given ± SEM, except for the average diameter (± SD); *n* values (number of independent measurements) are given in parentheses.

whereas complex synapses actually increased in number, reaching a maximum at 10 days postlesion. Thereafter, both types of synapse returned slowly to normal levels (3). The time course of the changes in PSD number for simple and complex synapses (Fig. 2) was identical to that for the synapses themselves except for a small number of vacated simple PSDs (PSDs unapposed by a presynaptic ending). The significant (4 days vs. unoperated, $P < 0.05$, $t = 2.9160$, df = 6) increase observed in the number of complex PSDs showed a delay of about 2 days with respect to the loss of simple PSDs, and the time course of increase in number of PSD perforations closely paralleled or slightly preceded the increase in complex PSDs (Fig. 2).

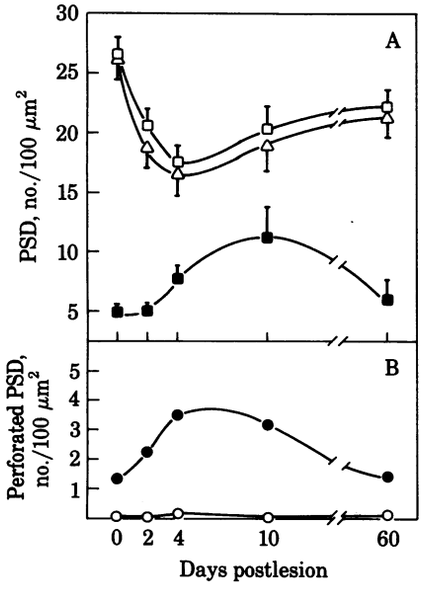

FIG. 2. Evolution of the number of PSDs and PSD perforations in the IML of the rat dentate gyrus after ipsilateral entorhinal ablation. (*A*) Number of simple (□) and complex PSDs (■). The number of complex synapses was identical to that of complex PSDs. The number of intact simple synapses (△) was slightly lower than that of PSDs due to the presence of a small proportion of "vacated" PSDs (i.e., PSDs without apposed presynaptic endings). (*B*) Number of perforated simple (○) and complex (●) PSDs. The SEM in *B* was smaller than the size of the symbols.

Balance of PSD Material in the DML Ipsilateral to an Entorhinal Lesion. The number of simple PSDs lost in the IML at 4 days postlesion was balanced by the number of complex PSDs gained by day 10 (Fig. 2), suggesting that simple PSDs were lost by becoming complex PSDs. Because complex PSDs are much larger than simple PSDs, the process of changing PSDs from simple into complex entailed the addition of a considerable amount of PSD material to the IML. With the data in Tables 2 and 3 and assuming that PSDs are disks of 30-nm average thickness, it was calculated that the total volume of complex PSD material in the IML increased 2.2-fold by 10 days after ipsilateral entorhinal ablation. This increase from 16.9×10^6 $nm^3/100$ μm^2 of tissue section (day 0) to 37.5×10^6 $nm^3/100$ μm^2 (day 10) began very early (2 days postlesion) and could have been due either to an increase in the rate of synthesis of new PSD components or to a transfer to the IML of material from disassembled PSDs in the MML and OML.

The ipsilateral MML and OML were directly denervated by the entorhinal ablation and lost 92% of their synapses and 46% of the PSDs 2 days after the lesion (refs. 14 and 15; Table 3). The dimensions of the remaining PSDs did not change significantly (Table 2) and the average PSD volume lost in the denervated areas by day 10 postlesion was -15.4×10^6 $nm^3/100$ μm^2. The overall volume of the total MML and OML was 2–2.5 times that of the IML. Therefore, approximately 2 times more PSD material seemed to be disassembled than appeared in the IML in complex PSDs. The PSD material thus lost could not be identified in discrete morphological entities within the neurons.

Ipsilateral MML and OML. Two days postlesion, only 8% of the total synapses in the outer two-thirds of the ipsilateral MML remained intact (14, 15). None of their PSDs was perforated. Those PSDs apposed to degenerating nerve endings and vacated PSDs were simple and showed no perforations. Reappearance of complex synapses in the MML and OML did

Table 2. Changes in the average diameter of PSDs in the dentate molecular layer ipsilateral to an entorhinal cortex ablation

Condition	Simple	Complex	Complex-P
	IML*		
Unoperated control	197 ± 57 (260)	321 ± 87 (33)	474 ± 118 (25)
Postlesion, time			
Day 2	201 ± 98 (355)	362 ± 115 (77)	480 ± 116 (23)
Day 4	211 ± 74 (327)	390 ± 122 (128)	504 ± 131 (43)
Day 10	199 ± 54 (191)	324 ± 85 (60)	462 ± 146 (38)
	MML*		
Unoperated control	204 ± 93 (263)	303 ± 71 (52)	443 ± 88 (28)
Postlesion, time			
Day 2	206 ± 80 (48)	298 ± 57 (11)	— (0)
Day 4	215 ± 77 (162)	312 ± 71 (38)	516 ± 142 (6)
Day 10	197 ± 53 (104)	355 ± 101 (35)	570 ± 126 (13)
	OML*		
Unoperated control	202 ± 57 (305)	336 ± 83 (66)	466 ± 85 (28)
Postlesion, time			
Day 2	206 ± 106 (68)	367 ± 104 (15)	— (0)
Day 4	237 ± 71 (81)	422 ± 37 (31)	— (0)
Day 10	209 ± 63 (99)	334 ± 78 (34)	451 ± 90 (7)

Simple, simple PSD; complex, complex PSD, nonperforated; complex-P, complex PSD, perforated. Values are the mean diameter ± SD of the n value of PSDs given in parentheses.
* Diameter of PSDs in each layer is given in nm.

not begin until day 10 postlesion (14). As reactive synaptogenesis proceeded, the fraction of complex synapses and that of perforated PSDs increased (significantly so at 60 days postlesion, $P < 0.01$, $t = 5.7341$, df = 5). The fraction of perforated PSDs reached its normal level at day 60 and did not exceed it thereafter.

DISCUSSION

We have studied the frequency of discontinuities (perforations) in dentate granule cell PSDs as a function of age and partial denervation and its relationship to synapse turnover in this brain area. Our data indicate that all the so-called complex synapses have perforated PSDs, whereas perforations are extremely rare in simple synapses. Accordingly, we propose that type I, or asymmetric, synapses can be subdivided into two further categories—those with perforations or discontinuities in the PSD and those without. Synapses with perforations in the PSD (complex synapses) are larger (average diameter = 480 nm; SD = 117 nm; n = 211) and less abundant than those without perforations. Perforated PSDs have distinctive population dynamics during synapse development and turnover. During development of the DML, complex PSDs appear after formation of simple synapses is essentially complete (17) and continue to increase until adulthood, and thereafter their proportion remains constant throughout adulthood and into old age (Table 1). When unilateral entorhinal ablation is used to induce nondegenerative synapse turnover in the ipsilateral dentate IML, a shift occurs in this brain area in the relative numbers of PSDs with and without perforations. Simple synapses are rapidly lost in the first 10 days after the lesion and their loss is followed by a corresponding increase in the number of complex synapses (Fig. 3). The inverse process predominates at later times (>10 days postlesion) when the number of complex synapses in the IML decreases and that of simple synapses increases. The reciprocal responses of simple and complex PSDs to the lesion are consistent with a precursor–product relationship between both synapse populations. This hypothesis is consistent with the striking increase in PSD material observed in the IML ipsilateral to an entorhinal ablation in spite of the large decrease in PSD numbers in the DML as a whole. Immunohistochemical staining of the hippocampus of lesioned animals with a PSD-specific antibody (18) also decreased in intensity in the MML

Table 3. Number of PSDs in the dentate molecular layer ipsilateral to an entorhinal lesion

	IML		OML*	
Condition	Simple	Complex	Simple	Complex
Unoperated control	28.2 ± 1.6	4.8 ± 0.7	31.8 ± 2.2	5.8 ± 1.2
Postlesion, time				
Day 2	21.1 ± 1.6	5.1 ± 0.8	15.9 ± 0.4	4.0 ± 0.2
Day 4	17.2 ± 1.7	7.9 ± 1.2	11.8 ± 0.7	5.7 ± 0.9
Day 10	20.4 ± 2.0	11.2 ± 2.7	18.3 ± 1.1	4.2 ± 0.8

Total PSDs in each category is the sum of PSDs in intact synapses, vacated PSDs, and PSDs apposed to a degenerating terminal. Values are the mean number of profiles ± SEM per 100 μm^2. Simple and complex are defined in Table 2.
* OML refers to the outer two-thirds of the molecular layer.

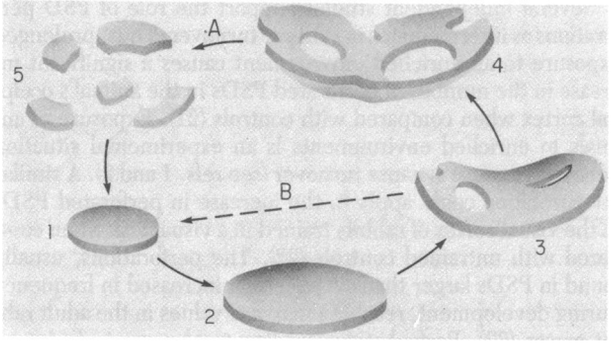

FIG. 3. The hypothetical life cycle of an asymmetric synapse in the dentate gyrus of the rat. The PSDs of simple synapses are small flat disks lacking perforations (1). Over time, their diameter increases by deposition of PSD components (2). When the PSDs reach a threshold size (or age) perforations, grooves, or tears appear (3) and grow or increase in number (or both) (4). The perforations cause the PSD to become a curved disk—a complex PSD. Finally, perforated PSDs break down into smaller fragments (5) (path A) that may give rise to a new simple PSD. Alternatively, the material lost from perforated PSDs either as individual molecules or as aggregates of them (i.e., coated vesicles) may be incorporated into nascent or mature PSDs (path B).

and OML but increased considerably in the IML by 3 days postlesion (19, 20).

There is increasing evidence that synapses are involved in a continuous turnover cycle (for reviews, see refs. 1 and 2) and the data discussed above can be interpreted in this context. We propose that the interconversion between nonperforated and perforated PSDs is an intermediate step in synapse breakdown and replacement. The hypothetical life cycle of a synapse is summarized in Fig. 3. Small simple PSD disks (no. 1 in Fig. 3) are synthesized in the course of synaptogenesis and with time grow larger by addition of PSD material (no. 2 in Fig. 3). As the size of the PSD grows, holes form (no. 3 in Fig. 3) and enlarge, weakening and distorting the junction (no. 4 in Fig. 3). Perforations may also develop like irregular grooves in the PSD surface, the deepening of which eventually tears the organelle. The presence of both types of PSD fragmentation—i.e., perforations and tears—has been observed in a serial section study in our laboratory. The final breakdown of complex PSDs may give rise to several PSD fragments (no. 5 in Fig. 3) one or more of which may give rise to a new simple synapse (path A) or, alternatively, the disassembled PSD material may be reassembled into new PSDs (path B). It is also conceivable that the PSD fragments in Fig. 3 could act as assembly nuclei for the new PSD.

If the sequence of events outlined above were correct, one would expect the average diameter of simple PSDs in the IML to increase shortly after an entorhinal lesion and subsequently return to normal as the larger simple PSDs become complex. The experimental findings were consistent with the hypothesis. Although the average diameter of simple PSDs (Table 2) did not change significantly, the diameter distribution at 2 and 4 days postlesion showed a significant increase in the population of diameters longer and shorter than the median when compared to unoperated controls (Mood test for equal medians: 2 days postlesion vs. unoperated, $z = 6.32$, $P < 0.000001$; 4 days postlesion vs. unoperated, $z = 6.08$, $P < 0.000001$). The distribution returned to that in unoperated animals by day 10 postlesion (Mood test: 10 days vs. unoperated, $z = 1.55$, $P > 0.05$). On the other hand, the average diameter of complex PSDs did not undergo distribution changes 2 days postlesion (Wilcoxon test for large samples: 2 days vs. unoperated, $z = -0.7$, $P > 0.05$) but shifted significantly towards longer lengths at 4 and 10 days postlesion (Mood test: 2 days vs. 4 days, $z = -2.21$, $P < 0.02$; 2 days vs. 10 days, $z = -2.83$, $P < 0.001$).

Several independent studies support the role of PSD perforations as intermediates in synapse turnover. Thus, prolonged exposure to an enriched environment causes a significant increase in the number of perforated PSDs in the animal's occipital cortex when compared with controls (21). Exposure of animals to enriched environments is an experimental situation believed to cause synapse turnover (see refs. 1 and 2). A similar interpretation could apply to the increase in perforated PSDs in the visual cortex of rabbits trained in a visual task when compared with untrained controls (22). The perforations, usually found in PSDs larger than average (22), increased in frequency during development, reaching maximal values in the adult rabbit cortex (23). Perturbations leading to changes in hormone levels also led to increased frequency of PSD perforations. Thus, in the paraventricular nucleus of the hypothalamus—a structure that controls the secretion of oxytocin and vasopressin—the frequency of PSD perforations was significantly higher in females that had borne offspring than in virgin animals (24), and ovariectomy had a similar effect on cortical synapses (25). Rats treated with increasing doses of anesthetic showed increasing numbers of complex PSDs (26–28), and it was suggested that synapses possessing complex PDSs (negatively curved) were nonfunctional (16), supporting our suggestion that perforated PSDs occur in synapses that are being disconnected.

If the premise that perforated PSDs are diagnostic of synapse turnover is accepted, then the proportion of synapses undergoing this process can be estimated. Thus, in the DML of young adult Sprague–Dawley rats, about 16% of the total PSD population are complex (i.e., perforated). Therefore, at any given time in the life of young adult laboratory rats, caged under standard conditions, 16% of their synapses in the DML are turning over. The proportion of synapses undergoing turnover and the rate at which the complete process takes place may vary considerably, depending on both physiological and environmental conditions and anatomical locus. In this context it is interesting to note that those areas of the brain known to be more plastic show a significantly higher proportion of perforated PSDs than hard-wired contacts. Thus, rabbit motor cortex shows a similar proportion of perforated PSDs (12–16% of the total) as the visual cortex (10–12%), whereas PSD perforations in the superior colliculi are much more scarce (3.7%) (22).

We are very grateful to Mr. R. B. Gibbs for writing the computer program for nonparametric statistics. This work was supported by grants from the National Institute of Aging (AG 00538) and from the National Institute of Mental Health (MH 19691).

1. Cotman, C. W. & Nieto-Sampedro, M. (1982) *Annu. Rev. Psychol.* **33**, 371–401.
2. Cotman, C. W., Nieto-Sampedro, M. & Harris, E. W. (1981) *Physiol. Rev.* **61**, 684–784.
3. Hoff, S. F., Scheff, S. W., Kwan, A. Y. & Cotman, C. W. (1981) *Brain Res.* **222**, 1–13.
4. Hoff, S. F., Scheff, S. W., Kwan, A. Y. & Cotman, C. W. (1981) *Brain Res.* **222**, 15–27.
5. Gray, E. G. (1959) *J. Anat.* **93**, 420–433.
6. Colonnier, M. (1968) *Brain Res.* **9**, 268–287.
7. Peters, A. & Kaisermann-Abramof, I. R. (1969) Z. *Zellforsch. Mikrosk. Anat.* **100**, 487–506.
8. Laatsch, R. H. & Cowan, W. M. (1966) *J. Comp. Neurol.* **128**, 359–396.
9. Cohen, R. S. & Siekevitz, P. (1978) *J. Cell Biol.* **78**, 36–46.
10. Cohen, R. S., Blomberg, F., Berzius, K. & Siekevitz, P. (1977) *J. Cell Biol.* **76**, 181–203.
11. Nieto-Sampedro, M., Bussineau, C. M. & Cotman, C. W. (1982) *J. Neurosci.* **2**, 722–734.
12. Blomberg, F., Cohen, R. S. & Siekevitz, P. (1977) *J. Cell Biol.* **74**, 204–225.
13. Cotman, C. W. & Nadler, J. V. (1978) in *Neuronal Plasticity*, ed. Cotman, C. W. (Raven, New York), pp. 227–271.
14. Hoff, S. F., Scheff, S. W., Bernardo, L. S. & Cotman, C. W. (1982) *J. Comp. Neurol.* **205**, 246–252.
15. Matthews, D. A., Cotman, C. W. & Lynch, G. (1976) *Brain Res.* **115**, 1–21.
16. Dyson, S. E. & Jones, D. G. (1980) *Brain Res.* **183**, 43–59.
17. Cotman, C., Taylor, D. & Lynch, G. (1973) *Brain Res.* **63**, 205–213.
18. Nieto-Sampedro, M., Bussineau, C. M. & Cotman, C. W. (1981) *J. Cell Biol.* **90**, 675–686.
19. Nieto-Sampedro, M., Bussineau, C. M. & Cotman, C. W. (1981) *Neurosci. Abstr.* **7**, 5.
20. Nieto-Sampedro, M., Bussineau, C. M. & Cotman, C. M. (1982) *Brain Res.*, in press.
21. Greenough, W. T., West, R. W. & De Voogd, T. J. (1978) *Science* **202**, 1096–1098.
22. Vrensen, G. & Nunes Cardozo, J. (1981) *Brain Res.* **218**, 79–97.
23. Muller, L., Pattisellano, A. & Vresen, G. (1981) *Brain Res.* **205**, 34–48.
24. Hatton, J. D. & Ellisman, M. H. (1982) *J. Neurosci.* **2**, 704–707.
25. Medosch, C. M. & Diamond, M. C. (1982) *Exp. Neurol.* **75**, 120–133.
26. Cooke, C. T., Nolan, T. M., Dyson, S. E. & Jones, D. G. (1974) *Brain Res.* **92**, 505–510.
27. Jones, D. G. & Devon, R. M. (1978) *Brain Res.* **147**, 47–63.
28. Jones, D. G. & Devon, R. M. (1977) *Neurosci. Lett.* **6**, 177–182.